Onset temperature of Bose-Einstein condensation in incommensurate solid ^{4}He

R. Rota and J. Boronat

Departament de Física i Enginyeria Nuclear, Campus Nord B4-B5,
Universitat Politècnica de Catalunya, 08034 Barcelona, Spain

(Dated: February 1, 2012)

Abstract

The temperature dependence of the one-body density matrix in ^{4}He crystals presenting vacancies is computed with Path Integral Monte Carlo. The main purpose of this study is to estimate the onset temperature T_0 of Bose-Einstein condensation in these systems. We see that T_0 depends on the vacancy concentration X_v of the simulated system, but not following the law $T_0 \sim X_v^{2/3}$ obtained assuming non-interacting vacancies. For the lowest X_v we have studied, that is $X_v = 1/256$, we get $T_0 = 0.15 \pm 0.05$ K, close to the temperatures at which a finite fraction of non-classical rotational inertia is experimentally observed. Below T_0, vacancies do not act as classical point defects becoming completely delocalized entities.

PACS numbers: 67.80.-s, 61.72.Bb

The debate about the supersolid state of matter, i.e., a phase where crystalline order coexists with superfluidity, has gained a great interest among the scientific community after the first observation of non classical rotational inertia (NCRI) in torsional oscillators containing solid helium [1, 2]. Although several experiments have confirmed the appearance of a phase transition in solid ^{4}He at temperatures $T_c \sim 60 - 100\,\mathrm{mK}$ [3, 4], we are still far from a complete description of this phenomenon because of controversial experimental results. For instance, the values of the superfluid density ρ_s/ρ reported so far can vary more than one order of magnitude according to experimental conditions such as the way in which the crystal is prepared, its subsequent annealing or the ^{3}He concentration [5–7]. These discrepancies suggest that the quality of the solid sample plays a very important role in these experiments and make fundamental a study of crystalline defects in quantum crystals.

First theoretical studies, indeed, suggested that a possible supersolid behavior can be explained assuming the presence, in the ground state of quantum crystals, of delocalized vacancies which may undergo Bose-Einstein condensation (BEC) at low temperature [8]. Nevertheless, these early works were based on simplified models, so that it was not possible to draw specific predictions for solid ^{4}He. More recently, microscopic methods have been extensively used to provide a reliable description of the supersolid state but, so far, they have not been able to reproduce all the experimental findings. Path integral Monte Carlo (PIMC) simulations have shown that a commensurate perfect crystal does not exhibit superfluidity [9–11], but a non-zero condensate fraction has been observed in crystals with a finite vacancy concentration at zero temperature [12].

The possibility for solid ^{4}He to present vacancies in its ground state seems to be hindered by the energetic cost of these defects. According to several Quantum Monte Carlo results, the vacancy formation energy is estimated to be of the order of 10 K [13–17], in agreement with experimental measurements [18]. Nevertheless, the high delocalization of the vacancies in solid ^{4}He at temperatures close to zero prevents an interpretation of these defects in terms of a classical theory involving an activation energy and a configurational entropy for their creation [19–21]. Furthermore, experimental data cannot rule out the possibility of a zero-point vacancy concentration below 0.4% [22]. It has also to be noticed that formation energy considerations do not exclude the possibility of vacancies introduced through the experimental conditions, for example during the crystal growth. The spatial correlation between vacancies has been calculated in order to understand if a gas of defects can be metastable in solid ^{4}He. The results show an attractive correlation between vacancies at short distance, but they cannot conclude if they form bound states and aggregate in large clusters which eventually would phase separate [14, 23–25].

In this work, we calculate by means of the Path Integral Monte Carlo (PIMC) method, the one-body density matrix $\rho_1(\mathbf{r}, \mathbf{r}')$ in solid ^{4}He samples presenting a finite vacancy concentration, focusing especially on its temperature dependence. In the study of the BEC properties of quantum systems, $\rho_1(\mathbf{r}, \mathbf{r}')$ is a fundamental quantity, the condensate fraction n_0 being its asymptotic limit for large $|\mathbf{r} - \mathbf{r}'|$ values. Our main purpose is to estimate the onset temperature of BEC T_0 and to compare it with the experimental measurements. We start simulating an hcp crystal with a vacancy concentration $X_v = 1/180$, trying also to give a qualitative picture of the delocalization of the vacancies and the appearance of BEC. Finally, we study the dependence of T_0 on X_v to guess which would be the vacancy concentration needed to have BEC appearing in the range of temperatures $T_c \sim 60 - 100\,\mathrm{mK}$ at which NCRI is experimentally observed.

PIMC provides a fundamental approach in the study of the thermodynamic properties of strongly interacting quantum systems at finite temperature [26]. In this method, the partition function Z is rewritten making use of the convolution property of the thermal density matrix $G(R', R; \beta) = \langle R'|e^{-\beta\hat{H}}|R\rangle$ (where $\beta = (k_B T)^{-1}$ is the inverse of the temperature and $\hat{H}$ is the Hamiltonian of the system), which is known only for small β. This procedure is equivalent to mapping the quantum many-body system at finite temperature onto a classical system of closed ring

polymers. Increasing the number of convolution terms used to rewrite Z, which corresponds to the number of beads composing each classic polymer, one is able to reduce the systematic error due to the approximation for G and therefore to recover "exactly" the thermal equilibrium properties of the system. A good approximation for the propagator G is fundamental in order to reduce the complexity of the calculation and ergodicity issues. Using the Chin approximation [27, 28], we are able to obtain an accurate estimation of the relevant physical quantities with reasonable numeric effort even in the low temperature regime, where the simulation becomes harder due to the large zero-point motion of particles. Chin approximation for the action is accurate to fourth order in the imaginary-time step but a real sixth-order behavior can be achieved by adjusting properly the two parameters entering in it. Similar accuracies can be achieved using other high-order proposals for the action [29–31].

An additional problem we have to deal with when approaching the low temperature limit with PIMC simulations arises from the indistinguishable nature of ^{4}He atoms. Since we study a bosonic system, the symmetry of Z can be recovered via the direct sampling of permutations between the ring polymers. To this purpose, we have used the Worm Algorithm [32]. This algorithm allows PIMC simulations with a very efficient sampling of the exchanges between bosons. Furthermore, it is able to give an estimation of the normalization factor of $\rho_1(\mathbf{r}_1, \mathbf{r}'_1)$, avoiding thus the systematical uncertainties which can be introduced by a posteriori normalization factor.

In order to calculate $\rho_1(r) = \rho_1(|\mathbf{r} - \mathbf{r}'|)$ in a crystal with vacancy concentration $X_v = 1/180$, we have carried out simulations of $N = 179$ ^{4}He atoms, interacting through an accurate Aziz pair potential [33], in an almost cubic simulation box matching the periodicity of an hcp lattice made up of $N_s = 180$ sites at a density $\rho = 0.0294$ Å^{-3}. We apply periodic boundary conditions to the simulation box in order to simulate the infinite dimensions of the bulk system. In Fig. 1, we show the results for $\rho_1(r)$ at different temperatures and we compare them with the zero temperature estimations of ρ_1 for the same system and for a perfect hcp crystal, obtained with the Path Integral Ground State method in Ref. [34]. We notice that, at temperatures $T \geq 0.75$ K, $\rho_1(r)$ computed in an incommensurate crystal, even though is not compatible with ρ_1 for the perfect crystal, presents a similar exponential decay at large r. At lower temperatures, the decay of $\rho_1(r)$ is smoother and, for temperatures $T \leq T_0 = 0.2$ K, ρ_1 presents a non-zero asymptote at large r, which indicates the presence of BEC inside the system. This T_0 can be considered a first estimate of the onset temperature of supersolidity in the simulated system. An analysis of the finite size effects would be needed to get a more precise estimation of the critical temperature of the supersolidity transition. Nevertheless, the simulation of bigger systems with exactly the same vacancy concentration requires a huge computational effort that would make the calculations impracticable.

In order to give a more qualitative description of the appearance of BEC in incommensurate ^{4}He solids, we visualize typical configurations of the system during the simulation. In Fig. 2, we plot two-dimensional projections of the positions of the quantum particles (represented by polymers in PIMC) lying in a basal plane of the incommensurate hcp crystal at different temperature. At $T = 1$ K, ^{4}He atoms tend to stay localized around their equilibrium positions. Also the vacancies are localized and can be easily detected inside the lattice. This explains the fact that, at that temperature, the presence of vacancies does not affect noticeably the overall behavior of ρ_1 which, for the incommensurate crystal, is similar to the one of the perfect crystal. At $T = 0.5$ K, the effects of the delocalization of the ^{4}He atoms can be seen with the appearance of some polymers which are spread on two different lattice points. In the space configurations at this temperature, the acceptance rate of the exchange between the polymers is higher than in the configurations at larger temperature, but it is still too low to allow the appearance of long permutation cycles, which are necessary to see BEC. At $T = 0.2$ K, the large zero-point motion of the ^{4}He atoms makes the vacancy delocalized and undetectable inside the crystal, which looks like a commensurate

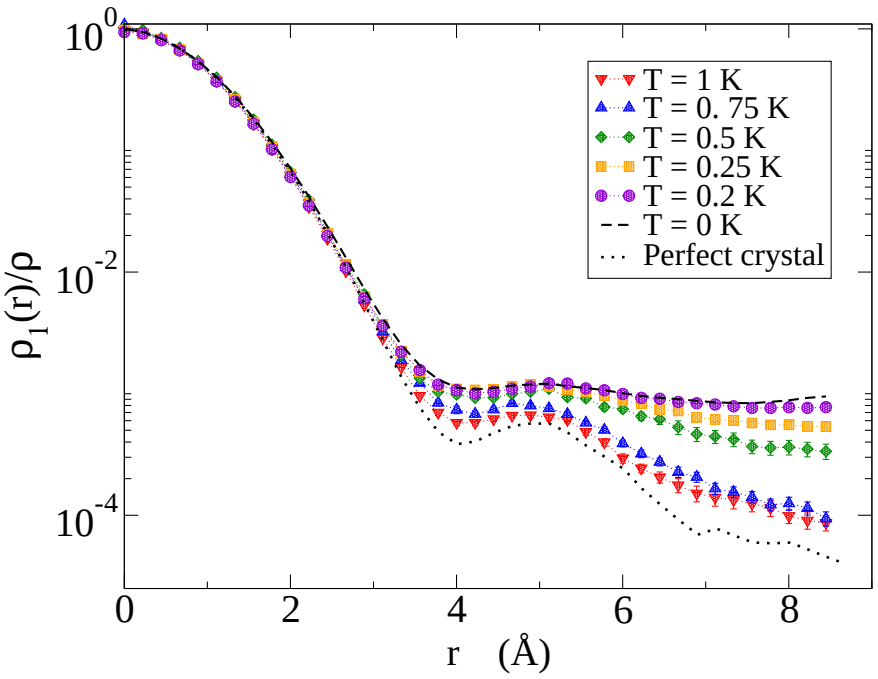

Figure 1: (Color online) The one-body density matrix $\rho_1(r)$ for an hcp crystal with vacancy concentration $X_v = 1/180$ at density $\rho = 0.0294$ Å^{-3} at different temperatures: $T = 1$ K (red triangles down), $T = 0.75$ K (blue triangles up), $T = 0.5$ K (green diamonds), $T = 0.25$ K (yellow squares) and $T = 0.2$ K (purple circles). The dotted and dashed lines represent $\rho_1(r)$ at zero temperature respectively for the commensurate ($X_v = 0$) and incommensurate crystal ($X_v = 1/180$) at the same density, taken from Ref. [34].

system. Since the number of lattice sites is different from the number of particles, this means that different polymers may superpose over the same lattice site: this occurrence strongly enhances the possibility for the atoms to permutate and allows the creation of long permutation cycles which close on periodic boundary conditions. The appearance of configurations presenting a non zero winding number, as the one shown in Fig. 3, indicates that the simulated crystals below $T_0 = 0.2$ K support superfluidity. However, it is not possible to give a reliable estimation for the superfluid density ρ_s/ρ in these systems, since the smallest value for ρ_s/ρ computable with the winding number estimator is of the order of 1%, that is of the same order of the value expected from the experimental measurements.

In order to study how the vacancy concentration in quantum solids affect the onset temperature of BEC, we have computed the one-body density matrix also for fcc ^{4}He crystals with $X_v = 1/108$, $X_v = 1/128$, and $X_v = 1/256$. It is worth noticing that the result for $X_v = 1/128$ has been obtained in a simulation with two vacancies in a lattice of 256 site points and the results for both the condensate fraction and onset temperature follow the same X_v dependence that the single vacancy cases. In Table I, we show the onset temperature of BEC T_0 and the condensate fraction n_0 at low temperature obtained with PIMC in the three crystals we have studied. We notice that, for the lowest X_v, we get $T_0 = 0.15 \pm 0.05$, which is close to the temperatures at which supersolidity has been experimentally observed.

In Fig. 4, we plot our results for T_0 as a function of X_v. Our results for T_0 do not follow the law $T_0 \sim X_v^{2/3}$, obtained from a description of solid ^{4}He in terms of a rarefied Gross-Pitaevskii superfluid gas of vacancies, as proposed by Anderson in Ref. [21]. This seems to suggest that, at least in the range of X_v we have been able to study, the correlations between vacancies have an important effect on T_0 and the system cannot be described within a mean-field approach.

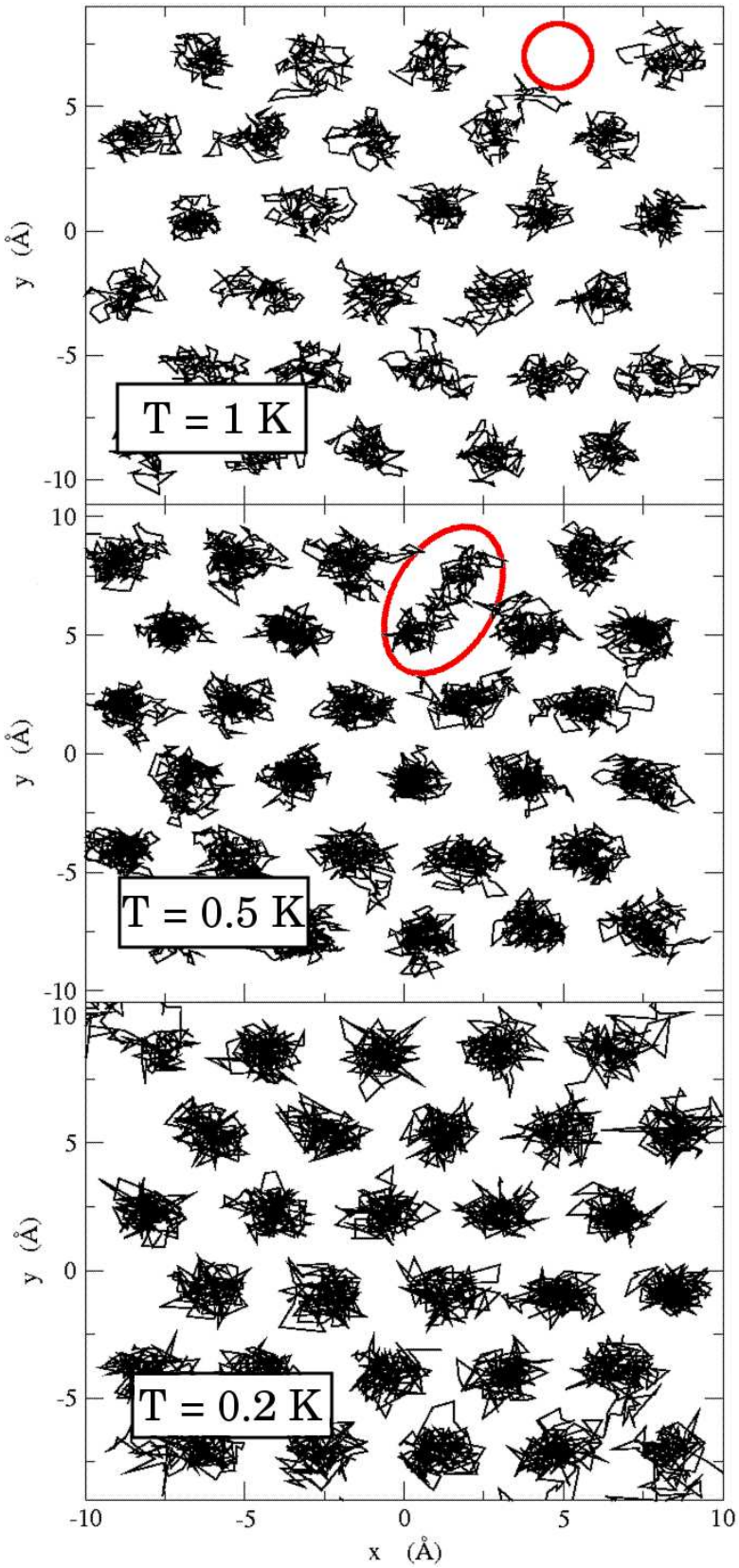

Figure 2: (Color online) Two-dimensional projection of basal planes of the incommensurate hcp crystal at different temperatures, represented according to the PIMC isomorphism of the classical polymers. At $T = 1$ K (higher panel) the vacancy is localized and indicated by the red circle. At $T = 0.5$ K (middle panel), the vacancy begins to delocalize: the red ellipse indicate a quantum particle delocalized over two different lattice sites. At $T = 0.2$ K (lower panel), the vacancy is completely delocalized and cannot be easily detected.

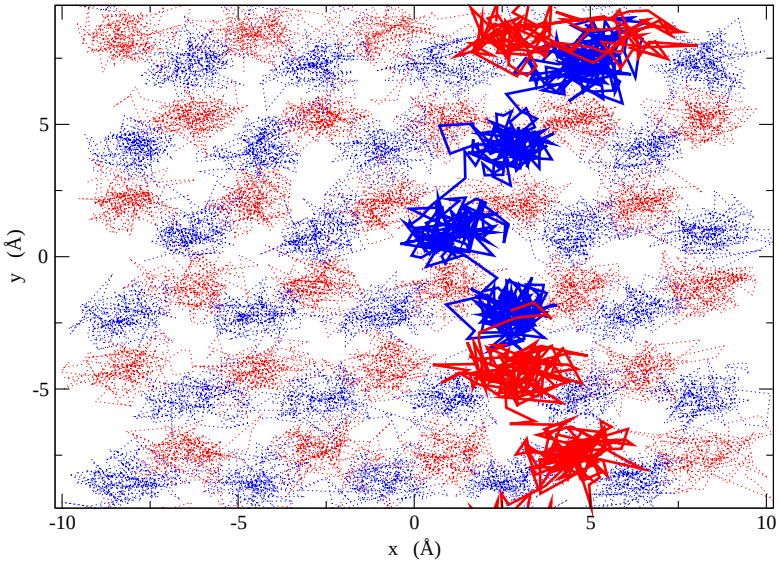

Figure 3: (Color online) Two-dimensional projection of two consecutive basal planes of the incommensurate hcp crystal at $T = 0.15$ K. The different colors distinguish the two different planes. The thick solid line represent a long permutation cycle between the ^{4}He atoms presenting a non-zero winding number.

N_v	N_s	X_v	T_0 (K)	n_0
1	108	1/108	0.50 ± 0.10	$(1.81 \pm 0.14)10^{-3}$
2	256	1/128	0.40 ± 0.075	$(1.09 \pm 0.13)10^{-3}$
1	180	1/180	0.20 ± 0.05	$(9.0 \pm 0.8)10^{-4}$
1	256	1/256	0.15 ± 0.05	$(7.2 \pm 0.8)10^{-4}$

Table I: The onset temperature of BEC T_0 and the condensate fraction n_0 at low temperature as a function of the vacancy concentration $X_v = N_v/N_s$, N_v and N_s being the number of vacancies and of lattice sites, respectively.

Nonetheless, our qualitative description of ^{4}He crystals supports the hypothesis [21] according to which it is not reasonable to regard vacancies in quantum solids as strictly local entities.

In an attempt to estimate which should be the vacancy concentration in ^{4}He crystals needed to have BEC appearing at the temperature T_c measured experimentally for the supersolid transition, we have plotted in Fig. 4 a power function trying to fit the PIMC results. According to this empirical law, ^{4}He crystals with a vacancy concentration $X_v \sim 2 - 3 \times 10^{-3}$ would have an onset temperature T_0 in agreement with the experimental values T_c. This result for X_v is in good agreement with the equilibrium vacancy concentration in solid ^{4}He at zero temperature obtained variationally with the shadow wave function [24].

In conclusion, we have shown that the onset temperature T_0 of BEC in ^{4}He crystals presenting vacancies, calculated using the PIMC method, is comparable with the experimental measurements of the supersolid transition temperature when the concentration of vacancies is small enough ($X_v \sim 2-3\times10^{-3}$). PIMC simulations also show clearly that when this onset temperature is reached the vacancies become completely delocalized objects, as hypothesized in the past [19, 21] and never microscopically observed so far.

This work was partially supported by DGI (Spain) under Grant No. FIS2008-04403 and Generalitat de Catalunya under Grant No. 2009-SGR1003.

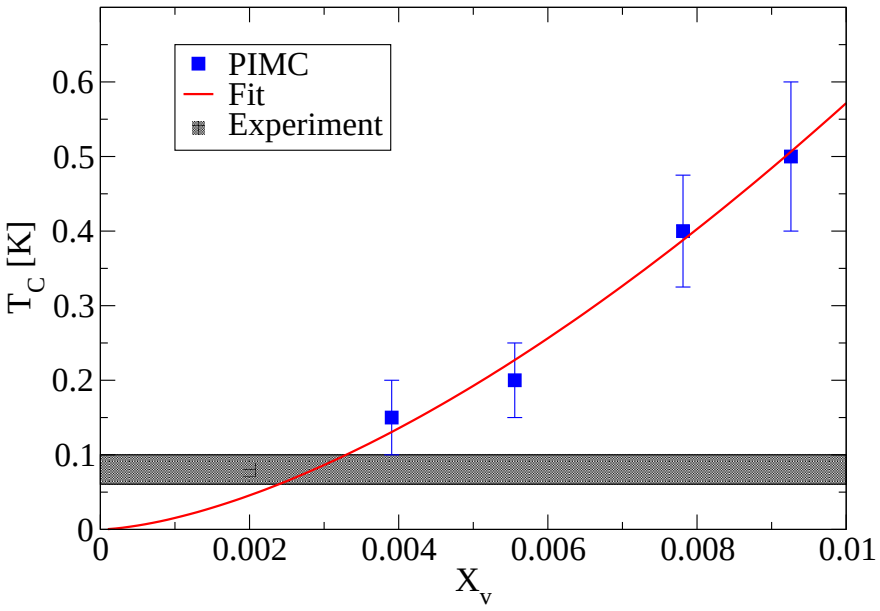

Figure 4: (Color online) The onset temperature T_0 of BEC in incommensurate solid ^{4}He as a function of the vacancy concentration X_v: the blue squares represent the results obtained with the PIMC method; the red line is a fit to the data with a power law $T_0 = AX_v^B$ with optimal values $A = 789$ K and $B = 1.57$; the grey band indicates the temperature at which the NCRI appears experimentally.

[1] E. Kim and M. H. W. Chan, Nature **427**, 225, (2004).
[2] E. Kim and M. H. W. Chan, Science **305**, 1941, (2004).
[3] Y. Aoki, J. C. Graves and H. Kojima, Phys. Rev. Lett. **99**, 015301, (2007).
[4] M. Kondo, S. Takada, Y. Shibayama, and K. Shirahama, J. Low. Temp. Phys. **148**, 695, (2007).
[5] A. S. Rittner and J. D. Reppy, Phys. Rev. Lett. **98**, 175302, (2007).
[6] A. Penzev, Y. Yasuta, M. Kubota, J. Low Temp. Phys. **148**, 677, (2007).
[7] A.C. Clark, J.T. West and M.H.W. Chan, Phys. Rev. Lett. **99**, 135302 (2007)
[8] A. F. Andreev and I. M. Lifshitz, Sov. Phys JEPT **29**, 1107, (1969).
[9] D. M. Ceperley and B. Bernu, Phys. Rev. Lett. **93**, 155303, (2004).
[10] B. K. Clark and D. M. Ceperley, Phys. Rev. Lett. **96**, 105302, (2006).
[11] D.E. Galli and L.Reatto, J. Phys. Soc. Jpn. **77**, 111010 (2008).
[12] D. E. Galli and L. Reatto, Phys. Rev. Lett. **96**, 165301, (2006).
[13] F. Pederiva, G.V. Chester, S. Fantoni, L. Reatto, Phys. Rev. B **56**, 5909 (1997)
[14] M. Boninsegni, A.B. Kuklov, L. Pollet, N.V. Prokof'ev, B.V. Svistunov and M.Troyer, Phys. Rev. Lett. **97**, 080401 (2006).
[15] B.K. Clark, D.M. Ceperley, Comput. Phys. Commun. **179**, 82 (2008).
[16] C. Cazorla, G. E. Astrakharchik, J. Casulleras, and J. Boronat, New. J. Phys. **11**, 013047, (2009).
[17] Y. Lutsyshyn, C. Cazorla, G. E. Astrakharchik, and J. Boronat, Phys. Rev. B **82**, 180506 (2010).
[18] B.A. Fraass, P.R. Granfors and R.O. Simmons, Phys. Rev. B **39**, 124 (1989).
[19] C. A. Burns and J. M. Goodkind, J. Low Temp. Phys. **95**, 695 (1994).
[20] P.W. Anderson, W.F. Brinkman, D.A Huse, Science **310**, 1164 (2005).
[21] P.W. Anderson, Science **324**, 631 (2009).
[22] R. Simmons and R. Blasdell, APS March Meeting, 2007 (unpublished).
[23] M. Rossi, E. Vitali, D.E. Galli, L. Reatto, J. Low Temp. Phys. **153**, 250 (2008).
[24] R. Pessoa, M. de Koning and S.A. Vitiello, Phys. Rev. B **80**, 172302 (2009).
[25] Y. Lutsyshyn, C. Cazorla, J. Boronat, J. Low Temp. Phys. **158**, 608 (2010)
[26] D. M. Ceperley, Rev. Mod. Phys. **67**, 279 (1995).

[27] S. A. Chin and C. R. Chen, J. Chem. Phys. **117**, 1409 (2002).
[28] K. Sakkos, J. Casulleras and J. Boronat, J. Chem. Phys. **130**, 204109 (2009).
[29] C. Predescu, Phys. Rev. E **69**, 056701 (2004).
[30] A. Balaz, A. Bogojević, I. Vidanović, and A. Pelster, Phys. Rev. E **79**, 036701 (2009).
[31] R. E. Zillich, J. M. Mayrhofer, and S. A. Chin, J. Chem. Phys. **132**, 044103 (2010).
[32] M. Boninsegni, N. V. Prokof'ev, B. V. Svistunov, Phys. Rev. E **74**, 036701 (2006).
[33] R. A. Aziz, F. R. W. McCourt, and C. C. K. Wong, Mol. Phys. **61**, 1487 (1987).
[34] R. Rota, J. Boronat, J. Low Temp. Phys. **162**, 146 (2011).